Fault Detection and Diagnosis of Permanent-Magnet DC Motor Based on Parameter Estimation and Neural Network

Xiang-Qun Liu, Hong-Yue Zhang, *Senior Member, IEEE*, Jun Liu, and Jing Yang

***Abstract*—In this paper, fault detection and diagnosis of a permanent-magnet dc motor is discussed. Parameter estimation based on block-pulse function series is used to estimate the continuous-time model of the motor. The electromechanical parameters of the motor can be obtained from the estimated model parameters. The relative changes of electromechanical parameters are used to detect motor faults. A multilayer perceptron neural network is used to isolate faults based on the patterns of parameter changes. Experiments with a real motor validate the feasibility of the combined use of parameter estimation and neural network classification for fault detection and isolation of the motor.**

***Index Terms*—Block-pulse function series, fault detection and diagnosis, neural network, parameter estimation, permanent-magnet dc motor.**

I. Introduction

LOW-POWER dc motors are widely used in industry and the military. Fault detection and diagnosis of dc motors in online monitoring and quality control have received growing attention among scientists and engineers.

A test system in online monitoring and quality control has to fulfill the following demands.

- The result of the diagnosis must describe the electromechanical behavior in detail. Faults must be detected and located precisely.
- In order to meet the demand for rapidity of online monitoring and high production rate, the diagnosis system must get results in a very short time.
- The easily measurable signals and simple sensors should be selected to cut down on the cost of the diagnosis system and its operation.

Nowadays, this kind of test is often done by a human tester or with conventional test techniques, but these methods do not fulfill all demands.

There have been many methods for fault detection and diagnosis of dc motors. These methods can be classified as methods based on signal analysis, methods based on motor dynamic model, and methods based on knowledge. It is known that each method has its own advantages and disadvantages. In the following, they are introduced respectively in brief.

Manuscript received January 15, 1999; revised April 29, 2000. Abstract published on the Internet July 1, 2000.

X.-Q. Liu, H.-Y. Zhang, and J. Yang are with the Department of Automatic Control, Beijing University of Aeronautics and Astronautics, Beijing 100083, China (e-mail: buaa301@mimi.cnc.ac.cn).

J. Liu is with China Hewlett-Packard Company, Ltd., Beijing 100022, China.

Publisher Item Identifier S 0278-0046(00)08833-X.

Firstly, methods based on signal analysis include vibration analysis [1], current analysis, [2], etc. These methods make use of signal models, such as spectrum, correlation function, and so on, to analyze the measured signals directly. Then, features of motor operating conditions can be extracted and used for motor fault detection and diagnosis. The main advantage of this kind of method is that accurate modeling of the motor is avoided. However, this kind of method only uses the output signals of motor, but no input signals, therefore, the influence of input on output is not considered. Hence, the dependence of output signals on input signals may be ignored. To a certain extent, the frequency analysis of measured signals is time consuming, so it is not suitable for the quick online test of a motor. Although vibration analysis is an effective method, it is difficult to get the reproducible diagnostic result due to the noise produced in environment and the coupling of the sensors to motor. Because of the noise and the high cost of accurate sensing devices, this method is usually considered useful for large motors only [15]. Additionally, the coupling of the sensors to motor influences the measurement of actual measured signal, in particular, when the transmission path effect on the actual measured signal cannot be ignored.

Secondly, methods based on a motor dynamic model include parameter estimation [3]–[5], state estimation [6]–[8], etc. This kind of method is able to perform online fault detection through the use of inexpensive monitoring devices that obtain the necessary measurements in a noninvasive manner. This kind of method makes use of both input and output signals of the motor adequately. However, its disadvantage is that it requires an accurate motor model. The parameter estimation method uses the undesired changes of physical parameters to detect and diagnose faults directly. Because of the obvious physical meaning of parameters, parameter estimation is of great advantage to fault isolation. One advantage of using a parameter estimation method is that a motor can be modeled accurately by balancing the equations. According to the magnitude of parameter change, the degree of seriousness of the fault can be estimated. However, it may be difficult to get the unique physical parameters according to the mapping relationship between the physical parameters and model parameters. The state estimation method makes use of predicted outputs from estimated motor states and actual measured outputs to generate residual series. By analyzing the information of faults included in the residual series, faults can be detected and diagnosed. When the state estimation method is used, the influence of large modeling error cannot be ignored. In addition, the noise

and the observability of state variables will influence the use of this method.

Thirdly, methods based on knowledge include methods based on expert system method, fuzzy logic and neural networks, etc. An expert system [11] can be built to detect and diagnose motor faults according to the experience accumulated by an experienced engineer, because an experienced engineer can detect and diagnose a motor fault by observing the motor operating behavior. The trouble with the use of this method is that accumulating experience and expressing it as knowledge rules are difficult and time consuming. Because a neural network has a strong ability for nonlinear function mapping, memorizing, fault tolerance, etc., it can be used for different purposes [7] [12]–[15]. For instance, a neural network can build the direct relationship between the measurements and faults [12]–[14] and it can be used to observe the motor state [7], [8], too, and so on. However, network training is time consuming, and the determination of network structure and the selection of a training sample are also difficult.

In order to fulfill motor fault detection and diagnosis, sometimes, several methods or their combination should be used. In this paper, the combination of *parameter estimation* method and *neural network* is adopted. Based on a linear continuous-time model of a permanent-magnet dc motor, the *block-pulse function series* method [9], [10] is used to estimate the parameter of the *continuous-time model* directly. A test bed is established to collect the input and output data of the dc motor. In the experiment, the input is input voltage increment, and output is speed increment and current increment. Only voltage, current, and speed are measured. Using the collected data and the method mentioned above, the parameters of a normal dc motor are estimated at first, and then different faults are injected into the motor, such as wear of the brush, opening of the coil, short circuit between adjacent commutator bars, etc. The parameter vectors estimated from the motor with faults then are compared with the parameters of the normal dc motor. Using the difference between the two sets of parameters, faults can thus be detected, and to some extent can be diagnosed.

Since one fault may cause variations of several parameters, sometimes, it is hard to isolate a fault by inspecting parameter variations directly. In order to diagnose the fault better, a *multilayer perception neural network* (MLPN) is used to classify the parameter variation patterns.

One of the main advantages of this diagnostic technique is that the parameters can be obtained easily without stopping the motor and without loading. The experimental results show that the combination use of parameter estimation and neural network classification is effective for fault detection and diagnosis of permanent-magnet dc motors.

II. Modeling of Permanent-Magnet DC Motor

In this section, the dynamic model of a permanent-magnet dc motor is first introduced. System identification theory is then applied to estimate the model parameters. The estimated model parameters are directly related to motor electromechanical parameters. Using the mapping relation between motor characteristics and electromechanical parameters, according to the estimated motor electromechanical parameters, fault detection can be performed in time.

Since the identification technique for a linear system is well established, a linear model is commonly used in practice. The process of establishing the linear dynamic model of a permanent-magnet dc motor is introduced in the following.

A. Nonlinear Dynamic Model of Permanent-Magnet DC Motor

The dynamic model of a permanent-magnet dc motor is given as follows:

$$\begin{cases} u = e_a + R_a i + L(i)\dfrac{di}{dt} \\ T = T_0 + T_2 + J\dfrac{d\Omega}{dt} \end{cases} \tag{1}$$

where u, e_a, i, R_a, and $L(i)$ are the armature voltage, back EMF, current, resistance, and inductance, respectively. Inductance $L(i)$ is the nonlinear function of current. T, T_0, and T_2 are the electromagnetic torque, no-load torque, and load torque, respectively. Ω is rotational speed (rad/s), J is the inertial moment of the rotator and load, and

$$e_a = C_e \Phi n = K_e n \tag{2}$$

$$T = C_T \Phi i = K_T i \tag{3}$$

where Φ is magnetic flux, and C_e, K_e, C_T, and K_T are coefficients.

Since T_0 is generated from the losses of the motor, it is very difficult to determine the value of T_0. T_0 can be expressed approximately as follows:

$$T_0 \approx T_0^* + T_r + T_p \tag{4}$$

where T_0^* is the friction torque, which is produced by the friction in the bearing or the friction between the brush and the commutator. T_0^* influences the motor startup characteristic and the startup voltage. T_r is affected by the bearing lubrication condition $T_r = f_r n$. T_p is produced by the aerodynamics, such as the resistance of the fan, etc., $T_p = f_p n^2$. Therefore,by using the relationship mentioned above, from (1), one can get

$$\begin{cases} u = K_e n + R_a i + L(i)\dfrac{di}{dt} \\ K_T i = T_0^* + f_r n + f_p n^2 + T_2 + J_1\dfrac{dn}{dt} \end{cases} \tag{5}$$

where n is the rotational speed (revolutions per minute), $n = 60\ \Omega/2\pi$, and $J_1 = (2\pi/60)J$.

It is well known that the operational characteristics of permanent-magnet dc motors can be obtained from (5), which have a direct mapping relation to the motor physical parameters, such as R_a, J, $L(i)$, etc. However, the relation between them is nonlinear. There are many nonlinear factors in the motor, for example, the nonlinearity of the magnetization characteristic of material, the effect of armature reaction, the effect caused by eddy current in the magnet, the residual magnetism, the commutator characteristic, mechanical friction, etc. Therefore, (5) is a nonlinear dynamic model.

B. Linear Dynamic Model of Permanent-Magnet DC Motor

To establish a linear dynamic model of a permanent-magnet dc motor, a linearization procedure is applied around some operation points.

At first, under no-load condition, $T_2 = 0$, and steady-state operation condition, $u(t) = u_0$, $i(t) = i_0$, and $n(t) = n_0$, one can get

$$\begin{cases} u_0 = K_e n_0 + R_a i_0 \\ K_T i_0 = T_0^* + f_r n_0 + f_p n_0^2 + T_2. \end{cases} \tag{6}$$

Suppose that the input voltage is changed from u_0 into $u_0 + \Delta u$, then motor speed and current are also changed as follows:

$$\begin{cases} n = n_0 + \Delta n \\ i = i_0 + \Delta i. \end{cases} \tag{7}$$

Substituting (7) into (5), one can obtain

$$\begin{cases} u_0 + \Delta u = K_e(n_0 + \Delta n) + R_a(i_0 + \Delta i) \\ \qquad + L\dfrac{d(i_0 + \Delta i)}{dt} \\ K_T(i_0 + \Delta i) = T_0^* + f_r(n_0 + \Delta n) + f_p(n_0 + \Delta n)^2 \\ \qquad + T_2 + J_1\dfrac{d(n_0 + \Delta n)}{dt} \end{cases} \tag{8}$$

where $L = L(i_0)$ is a constant [in the following L is used instead of $L(i_0)$]. Subtracting (6) from (8), neglecting the terms $2f_p n_0 \Delta n$ (f_p is small) and $f_p \Delta n^2$, then the linear dynamic model of motor is obtained as

$$\begin{cases} L\dfrac{d\Delta i}{dt} = \Delta u - K_e \Delta n - R_a \Delta i \\ J_1\dfrac{d\Delta n}{dt} = K_T \Delta i - f_r \Delta n. \end{cases} \tag{9}$$

For clarity of notation, Δu, Δi, and Δn in (9) are replaced, respectively, by u_Δ, i_Δ, and n_Δ. Then, (9) can be written as follows:

$$\begin{cases} L\dfrac{di_\Delta}{dt} = u_\Delta - K_e n_\Delta - R_a i_\Delta \\ J_1\dfrac{dn_\Delta}{dt} = K_T i_\Delta - f_r n_\Delta. \end{cases} \tag{10}$$

Equation (10) can be written in state-space form as follows:

$$\begin{bmatrix} \dot{i}_\Delta(t) \\ \dot{n}_\Delta(t) \end{bmatrix} = \begin{bmatrix} -R_a/L & -K_e/L \\ K_T/J_1 & -f_r/J_1 \end{bmatrix} \begin{bmatrix} i_\Delta(t) \\ n_\Delta(t) \end{bmatrix} + \begin{bmatrix} 1/L \\ 0 \end{bmatrix} u_\Delta(t)$$

or

$$\dot{X}(t) = AX(t) + BU(t) \tag{11}$$

where

$$X(t) = \begin{bmatrix} i_\Delta(t) \\ n_\Delta(t) \end{bmatrix}$$

$$A = \begin{bmatrix} -R_a/L & -K_e/L \\ K_T/J_1 & -f_r/J_1 \end{bmatrix}$$

$$B = \begin{bmatrix} 1/L \\ 0 \end{bmatrix}$$

$$U(t) = [u_\Delta(t)].$$

Matrices A and B are related to motor electromechanical parameters (R_a, L, K_T, K_e, f_r, and J_1) directly.

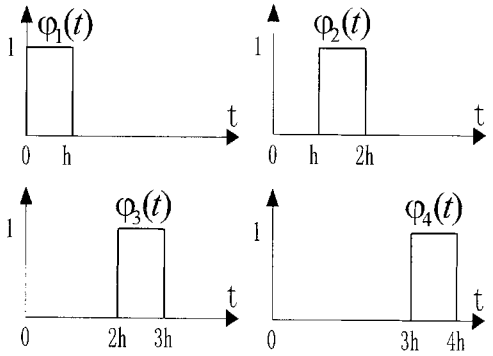

Fig. 1. Block-pulse function series.

III. Parameter Estimation of Continuous-Time System

A common approach to estimate system parameters is to transfer the continuous-time differential equation (11) into a discrete-time difference equation first, then apply a parameter estimation algorithm, such as the least-squares method, to estimate parameters of the discrete-time system, and finally transfer the discrete-time system parameters back into continuous-time system parameters. Such approach involves two transformations. It is not only time consuming in computation time, but also causes degradation of estimation accuracy.

Therefore, it is advantageous to use algorithms directly to estimate parameters of continuous-time systems. At the same time, this method will keep the physical meaning of parameters unchanged. There are many such algorithms proposed, e.g., orthogonal function series approach, state filter approach, etc. Here, the former approach, specifically block-pulse function series, is adopted.

A. Block-Pulse Function Series and its Application to Continuous-Time System Identification

For the time being, assume that the initial condition $X(0)$ of (11) is zero. Integrating both sides of (11), one obtains

$$X(t) = A\int_0^t X(t)\,dt + B\int_0^t u_\Delta(t)\,dt. \tag{12}$$

Now, the block-pulse function series $\Phi(t)$ is used to approximate $X(t)$, $u_\Delta(t)$, and their integrals

$$\Phi(t) = [\varphi_1(t),\, \varphi_2(t),\, \cdots,\, \varphi_m(t)]^T. \tag{13}$$

$\Phi(t)$ is shown in Fig. 1, where $m = 4$, $h = T/m$ is the step size or sampling period, and T is the duration of approximation.

$u_\Delta(t)$ can be approximated using $\Phi(t)$ as follows:

$$u_\Delta(t) \cong u_1\varphi_1(t) + u_2\varphi_2(t) + \cdots + u_m\varphi_m(t) = F_u^T\Phi(t) \tag{14}$$

where

$$F_u^T = [u_1,\, u_2,\, \cdots,\, u_m],$$

$$u_k = \frac{1}{2}[u_\Delta(kh - h) + u_\Delta(kh)], \qquad k = 1,\, 2,\, \cdots,\, m.$$

$u_\Delta(t)$ and its block-pulse function series approximation are shown in Fig. 2.

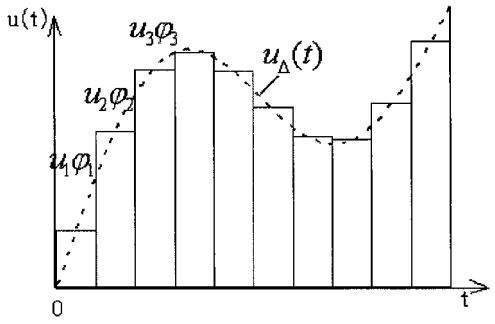

Fig. 2. Functional approximation using block-pulse function.

Similarly, one has

$$i_\Delta(t) \cong i_1\varphi_1(t) + i_2\varphi_2(t) + \cdots + i_m\varphi_m(t) = F_i^T\Phi(t) \tag{15}$$

$$n_\Delta(t) \cong n_1\varphi_1(t) + n_2\varphi_2(t) + \cdots + n_m\varphi_m(t) = F_n^T\Phi(t) \tag{16}$$

where

$$F_i^T = [i_1, i_2, \cdots, i_m],$$
$$i_k = \frac{1}{2}[i_\Delta(kh-h) + i_\Delta(kh)], \qquad k = 1, 2, \cdots, m$$
$$F_n^T = [n_1, n_2, \cdots, n_m],$$
$$n_k = \frac{1}{2}[n_\Delta(kh-h) + n_\Delta(kh)], \qquad k = 1, 2, \cdots, m.$$

Let C and D be output and input matrices of the motor, respectively,

$$C = \begin{bmatrix} i_1 & i_2 & \cdots & i_m \\ n_1 & n_2 & \cdots & n_m \end{bmatrix} = \begin{bmatrix} F_i^T \\ F_n^T \end{bmatrix} \in R^{2\times m}$$
$$D = [u_1 \;\; u_2 \;\; \cdots \;\; u_m] = [F_u^T] \in R^{1\times m}.$$

Then,

$$X(t) = C\Phi(t) \tag{17}$$
$$u_\Delta(t) = D\Phi(t). \tag{18}$$

Substituting (17) and (18) into (12), one obtains

$$C\Phi(t) = AC\int_0^t \Phi(t)\,dt + BD\int_0^t \Phi(t)\,dt. \tag{19}$$

From $\Phi(t) = [\varphi_1(t), \varphi_2(t), \cdots, \varphi_m(t)]^T$, one can get

$$\int_0^t \Phi(t)\,dt = H\Phi(t) \tag{20}$$

where

$$H = h\begin{bmatrix} 1/2 & 1 & \cdots & 1 \\ \cdots & 0 & \ddots & \ddots & \vdots \\ & \vdots & \ddots & \ddots & 1 \\ & 0 & \cdots & 0 & 1/2 \end{bmatrix} \in R^{m\times m}.$$

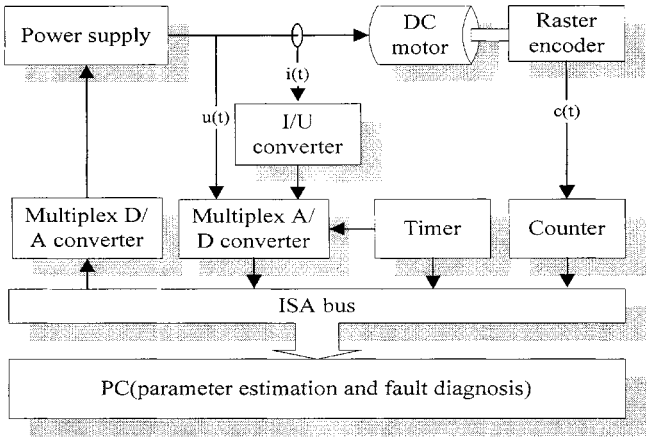

Fig. 3. Motor test-bed diagram.

Therefore, (19) can be transformed into the following algebraic equation:

$$C\Phi(t) = ACH\Phi(t) + BDH\Phi(t). \tag{21}$$

Canceling $\Phi(t)$ on both sides of (21), one gets

$$C = \theta Z \tag{22}$$

where $\theta = [A \;\; B] \in R^{p(p+q)}$, $Z = \left[\begin{smallmatrix} CH \\ DH \end{smallmatrix}\right] \in R^{(p+q)m}$, p is the dimension of system state, and q is the dimension of input. In the present case, $p = 2$, and $q = 1$.

When $m > p(p+q)$, least-squares method can be used to estimate θ and obtain

$$\hat{\theta} = CZ^T(ZZ^T)^{-1}. \tag{23}$$

If $X(0) \neq 0$, from (11), one gets

$$X(t) - X(0) = A\int_0^t X(t)\,dt + B\int_0^t u_\Delta(t)\,dt. \tag{24}$$

Using block-pulse function series to transform (24), one can get

$$C\Phi(t) - E\Phi(t) = ACH\Phi(t) + BDH\Phi(t) \tag{25}$$

where $C$and $D$are the same as before, and E is the initial state matrix, $E = \left[\begin{smallmatrix} i(0)\; i(0) \cdots i(0) \\ n(0)\; n(0) \cdots n(0) \end{smallmatrix}\right] \in R^{2\times m}$.

The least-squares estimation can be written as

$$\hat{\theta} = (C - E)Z^T(ZZ^T)^{-1}. \tag{26}$$

Thus, the model parameters can be identified. A recursive formula of identification using block-pulse function series method can also be used [10].

B. Motor Fault Detection Based on Parameter Estimation

At first, it is verified by simulation that the parameter estimation method based on block-pulse function series can be used to estimate the parameters of the continuous-time model of a permanent-magnet dc motor directly. Then, experiments are conducted to estimate the parameters of a motor using experimental data.

In the experiment, the input of the motor is a step voltage, and the data of voltage, current, and speed can be collected under no-load condition by the motor test bed. By using the

TABLE I
TECHNICAL PARAMETERS OF THE TESTED MOTOR

Nominal power P_N	$120w$	Back-emf coefficient K_e	8.57×10^{-3} V/rpm
Nominal voltage U_N	$24V$	Rotor inertia J	1.42×10^{-5} N.M.S
Resistant R_a	1.21Ω	Friction coefficient f_r	2.45×10^{-5} N.M/rpm
Inductance L	5.84×10^{-3}H		

TABLE II
FAULT TYPES AND INJECTION METHODS

Fault No.	Fault Type	Fault Injection Method
0	Fault free	None
1	Increase of armature resistance	Add resistance of 0.5 Ω
2	Increase of armature resistance	Add resistance of 1.14 Ω
3	Wearing of brush, insufficient brush pressure	Use worn brush, relax brush spring
4	Opening of coil	Open one coil
5	Short circuit of two commutator bars	Connect two adjacent bars of commutator
6	Disconnection of coil from commutator bar	Disconnect coil from commutator bar

TABLE III
PARAMETER ESTIMATION OF FAULT-FREE AND FAULTY MOTOR

Fault No.	R_a (Ω)	$L_{\times10^{-3}}$ (H)	$K_{e\times10^{-3}}$ (V/rpm)	$J_{\times10^{-5}}$ (N.M.S)	$f_{r\times10^{-5}}$ (N.M/rpm)
0	1.2030	5.5840	8.5740	1.4166	2.4500
1	1.7725	5.5837	8.3988	1.3949	2.4891
2	2.2837	6.4942	8.4921	1.5188	2.0201
3	1.7690	6.0798	9.2140	1.5670	2.4682
4	1.7945	5.7591	8.6391	1.5686	2.4530
5	1.1743	4.4053	7.3402	1.2214	4.0144
6	1.4365	8.7548	8.0655	1.4854	4.3227

method mentioned above, first the parameters of the motor in the normal case are estimated, then different faults are injected into the motor and the parameters of the faulty motor are estimated. Comparing the estimated parameters of the faulty motor with the estimated parameters of the normal motor, one can detect the motor faults.

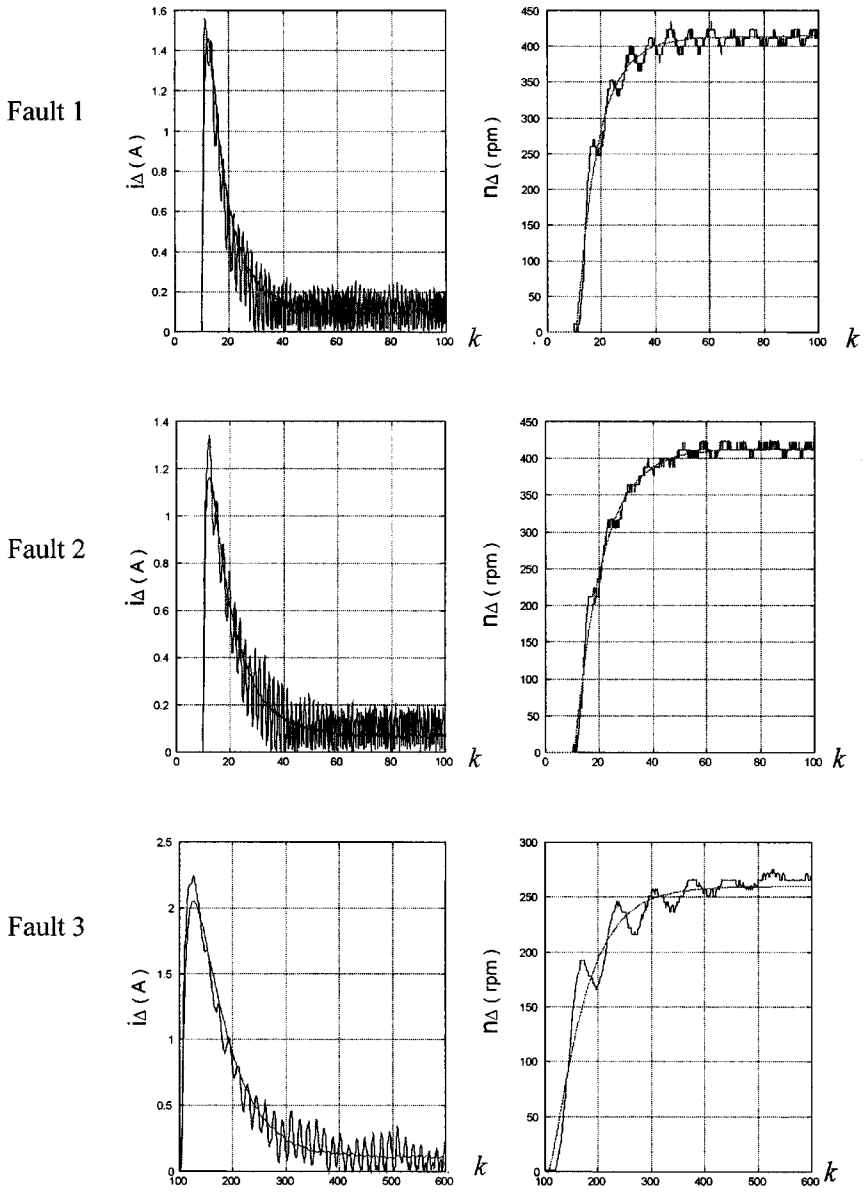

Fig. 4. Outputs of motor and identified model under different faults.

1) Experiment of Motor Fault Detection Based on Parameter Estimation: The diagram of the motor test bed is shown in Fig. 3. Motor armature current $i(t)$ is measured using an I/U converter. Motor rotational speed $n(t)$ is calculated using the output pulses $c(t)$ from the raster encoder. The motor used in the test is a type of low-power permanent-magnet dc motors. The technical parameters of the tested motor are listed in Table I.

In the experiment, firstly, an increment voltage $u_{\Delta}(t) = 4$ V from the operating point, which is different from the nominal operating point, is applied to the motor, and the corresponding increments of current $i_{\Delta}(t)$ and speed $n_{\Delta}(t)$ of the motor are calculated according to the collected current $i(t)$ and speed $n(t)$, then the above parameter estimation method is used to get the parameters in the fault-free case. Secondly, six faults listed in Table II are injected into the motor. The parameters in different fault cases are estimated by using the same method, then they are compared with the parameters of the normal dc motor. Using the difference between the two sets of parameters, faults can, thus, be detected, and to some extent can be diagnosed.

According to the mentioned algorithm and the experiment data of the same motor with different faults, the results of estimated motor electromechanical parameters are listed in Table III.

Fig. 4 shows outputs (fluctuant curves) of the motor with different faults and outputs (smooth curves) of the model with the estimated parameters listed in Table III. In Fig. 4, k is the sampling step, and the sampling period is 0.5 ms.

It can be seen from Fig. 4 that model outputs approximate the average values of motor outputs quite well in all cases, which means the result of parameter estimation is good. Table IV shows the relative changes of parameter estimates in different fault cases, where

$$\varepsilon_j = \frac{\hat{p}_j - p_{oj}}{p_{oj}}, \qquad j = 1, 2, \cdots, 5. \tag{27}$$

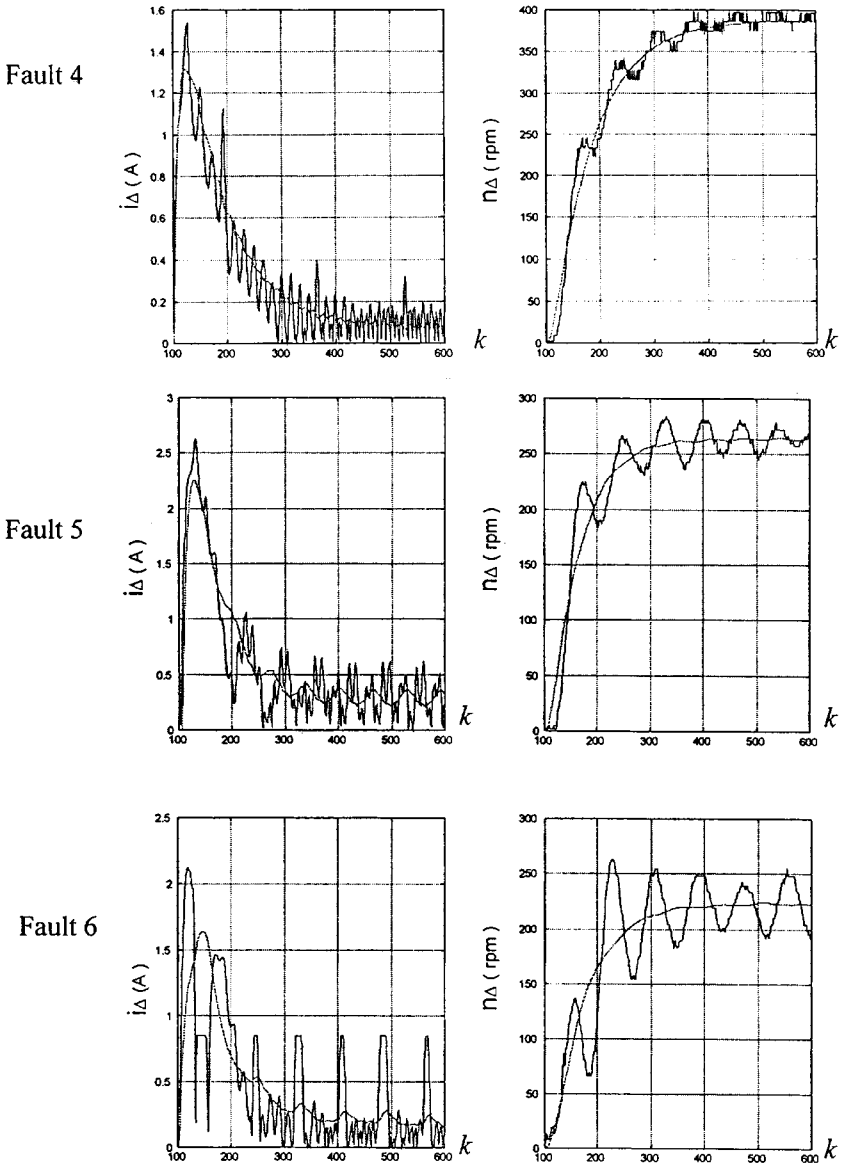

Fig. 4. *(Continued.)* Outputs of motor and identified model under different faults.

$\hat{p}_j$ is the estimated parameter of the faulty motor, and p_{oj} is the estimated parameter of the normal motor.

The changes of parameters form different patterns for each fault case and are depicted in Fig. 5.

2) Analysis of Experiments and Fault Detection Results: From the Tables III and IV, it can be seen that, in the first case of fault, the armature resistance increases 0.5 Ω, the estimated resistance increases 0.5695 Ω, and its relative change $\varepsilon_{Ra} = 0.4734$. Relative changes of other parameters are very small. In the second case of fault, the result is similar to that of the first case. However, because ε_{Ra} is twice as large as before, the armature current decreases considerably, and it deviates from the operation point of motor considerably, therefore, ε_L and ε_{fr} become larger than in the first case.

In the third case of fault, ε_{Ra} is also the largest one; other parameters also have some degree of change.

In the fourth case of fault, under the condition of pole pair number $p = 1$, opening one circuit will change the number of the shunt-wound circuit, ε_{Ra} increases to 50%, and ε_{Ke} is almost zero.

In the fifth case of fault, because of the local short circuit of two adjacent commutator bars, the armature circuit is unbalanced. It causes the vibration of current and speed, and ε_{fr} becomes the largest one, $\varepsilon_{fr} = 0.6835$.

The sixth case is similar to the fifth case. Because of the local open circuit, the vibration of current and speed is serious, and ε_{fr} is the largest one, $\varepsilon_{fr} = 0.7644$.

It is clear that motor faults will cause motor parameters to change, therefore, it is easy to detect a motor fault by comparing its estimated parameters with normal parameters. When parameter change exceeds a preset threshold, a fault is immediately detected. Because the pattern of parameter changes is different for different faults, the pattern classification method is suggested to isolate the motor faults. However, one fault may cause many parameters to change, therefore, isolating the fault is not easy by just looking at the pattern of parameter changes in Fig. 5. In

TABLE IV
RELATIVE CHANGES IN PARAMETER ESTIMATES FOR THE FAULTY MOTOR

Fault No.	ε_{Ra}	ε_{L}	ε_{Ke}	ε_{J}	ε_{fr}
1	0.4734	0.0006	-0.0204	-0.0153	0.0160
2	0.8983	0.1630	-0.0096	0.0721	-0.1755
3	0.4705	0.0888	0.0746	0.1062	0.0074
4	0.4917	0.0314	0.0076	0.1073	0.0012
5	-0.0239	-0.2111	-0.1439	-0.1378	0.6385
6	0.1941	0.5678	-0.0592	0.0486	0.7644

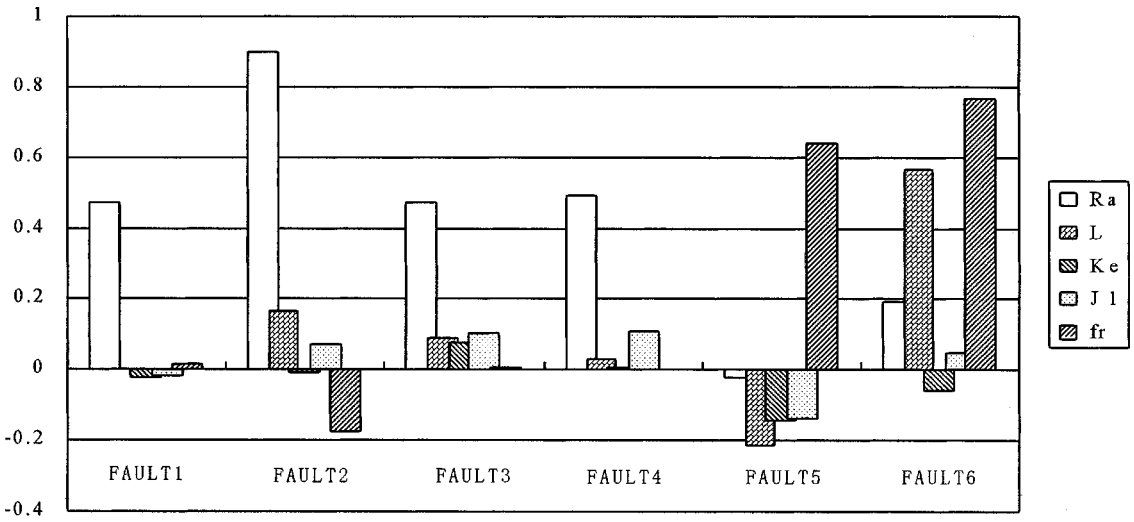

Fig. 5. Relative change in parameter estimates for faulty motor.

order to isolate the faults, the classification ability of a neural network is used.

IV. MOTOR FAULT ISOLATION USING NEURAL NETWORK

Fault isolation is a mapping from fault symptoms to fault causes. There are many ways to do the mapping, such as expert system, fuzzy logic reasoning, neural network, etc., or some combination of several methods. Here, the neural network approach is adopted, and an MLPN is selected for the purpose of fault classification.

The MLPN consists of an input layer, output layer, and two hidden layers. The input layer has five neurons corresponding to five motor parameters. The output layer has seven neurons corresponding to one fault-free case and six fault cases. The first hidden layer has eight neurons and the second layer ten neurons.

The training input samples are the relative change of parameters ε_j (in Table IV). In order to consider the noise effect, and make the network output robust to noise, $\pm 5\%$ change is added to oneε_j ($j = 1, 2, \cdots, 5$) and the others are unchanged. Therefore, an additional ten samples are obtained. Altogether, there are 11 samples.

The training output samples are listed in Table V. The first row corresponds to the fault-free case, while the ith row corresponds to the $(i-1)$th fault, $i = 2, \cdots, 7$.

Error backpropagation with a momentum term is adopted as the training algorithm. The criterion for training is

$$E = \frac{1}{N}\sum_{p=1}^{N} E_p \tag{28}$$

where N is the number of samples (in the simulation $N = 11$)

$$E_p = \frac{1}{n}\sum_{i=0}^{n} E_{pi} \tag{29}$$

where n is the number of faults (in the simulation $n = 6$)

$$E_{pi} = \tfrac{1}{2}\sum_{k=1}^{M}(O_{pki} - y_{pki})^2 \tag{30}$$

where M is the number of output neurons (in the simulation $M = 7$), O_{pki} is the expected output of the kth neuron, and

TABLE V
TRAINING OUTPUT SAMPLES

Fault No.	Neuron Output						
	Neuron 1	Neuron 2	Neuron 3	Neuron 4	Neuron 5	Neuron 6	Neuron 7
0	1	0	0	0	0	0	0
1	0	1	0	0	0	0	0
2	0	0	1	0	0	0	0
3	0	0	0	1	0	0	0
4	0	0	0	0	1	0	0
5	0	0	0	0	0	1	0
6	0	0	0	0	0	0	1

TABLE VI
RESULTS OF FAULT ISOLATION

Output / Fault No	Y1	Y2	Y3	Y4	Y5	Y6	Y7
0	0.992	0.009	0.000	0.000	0.008	0.0005	9e-6
1	0.003	0.986	0.000	2e-6	7e-6	0.011	0.005
2	0.000	0.000	0.989	0.008	0.000	8e-6	1e-4
3	0.000	0.000	0.005	0.989	0.000	0.011	0.004
4	0.005	0.000	0.000	0.000	0.992	0.000	0.004
5	0.000	0.028	0.000	0.004	1e-6	0.991	0.003
6	0.000	0.003	0.000	9e-5	0.004	0.002	0.991

y_{pki} is the actual output. When $E < 0.005$ or the number of training epochs $K > 5000$, the training stops.

After the training, the values in Table IV are used as input samples. The outputs of the network are listed in Table VI. The isolation criterion is

$$F_j = \{j | Y_j = \max(Y_1, Y_2, \cdots, Y_M)\} \tag{31}$$

where $Y_i (i = 1, 2, \cdots, M)$ is the output of the neural network. As can be seen from Table VI, the results of isolation for every fault are very accurate.

V. CONCLUSIONS

From the above discussion and the results, the following conclusions can be drawn.

1) It has been shown by theoretical derivation, simulation, and experiment that a parameter estimation method based on block-pulse function series can be used directly to estimate the parameters of the continuous-time model of a permanent-magnet dc motor. These model parameters can be easily converted to the motor electromechanical parameters according to the relation given by the motor model.
2) By comparing the relative changes of electromechanical parameters due to faults with a preset threshold, the faults can be detected. The magnitude of parameter change is also a direct indication of the degree of seriousness of the fault. Different faults may result in different patterns of parameter changes. If one fault causes one parameter change, using this one-to-one mapping, the fault is easily isolated from the specific parameter change. Gen-

erally speaking, one fault may cause many parameters to change. Due to this one-to-many mapping, it is difficult to isolate a fault by just looking at many parameter changes. However, the pattern of parameter changes is different for different faults. A pattern classification method has been suggested to isolate the motor faults.

3) A neural network has a good ability for pattern classification. An MLPN has been adopted to isolate the faults of the permanent-magnet dc motor. Experimental results have shown that the isolation of motor faults is quite good.
4) The test bed, which does not use the clutch to connect the motor to a brake, is simple and inexpensive. Only voltage, current, and speed are measured in the experiment. To make the parameter estimation successful, it is important to collect the input and output data of the motor accurately. Therefore, the test bed of the motor should be calibrated carefully.

REFERENCES

[1] D. Filbert, "Intelligent measurement methods in technical diagnosis and quality assurance—A comparison," *Measurement*, vol. 6, no. 2, pp. 69–74, 1988.

[2] R. R. Schoen, T. G. Habetler, F. Kamran, and R. G. Bartheld, "Motor bearing damage detection current monitoring," *IEEE Trans. Ind. Applicat.*, vol. 31, pp. 1274–1279, Nov./Dec. 1995.

[3] D. Filbert, "Advanced faulty diagnosis for the mass production of small power electric motors," in *Proc. Electro Motion 2*, 1995, pp. 159–166.

[4] C. Schneider and D. Filbert, "Parameter estimation and residual analysis a comparison," in *Proc. IFAC Fault Detection, Supervision and Safety for Technical Processes*, Espoo, Finland, 1994, pp. 701–705.

[5] R. Isermann, "Process fault detection and diagnosis methods," in *Proc. IFAC Fault Detection, Supervision and Safety for Technical Processes*, Espoo, Finland, 1994, pp. 597–612.

[6] K. Watanabe, M. Sasak, and D. M. Himmelblan, "Determination of optimal measuring sites for fault detection of nonlinear systems," *Int. J. Syst. Sci.*, vol. 16, pp. 1345–1363, 1985.

[7] K.-S. Lee, J.-S. Ryu, and T.-G. Park, "An intelligent fault detection and isolation scheme for a class of nonlinear systems," in *Proc. 2nd Asian Control Conf.*, Seoul, Korea, July 1997, pp. III-83–III-86.

[8] C. W. Chan, K. C. Cheung, H. Y. Zhang, and Y. Wang, "Fault detection of DC-motors using nonlinear observer based on recurrent B-spline neurofuzzy network," in *Proc. 14th IFAC World Congr.*, vol. B, Beijing, China, 1999, pp. 511–516.

[9] H. Y. Zhang and J. Chen, "Identification of stochastic multi-variable continuous-time systems," *Int. J. Modeling Simulation*, vol. 10, no. 2, pp. 71–74, 1990.

[10] ——, "Identification of physical parameters of ground vehicle using block-pulse function method," *Int. J. Syst. Sci.*, vol. 21, no. 4, pp. 631–642, 1990.

[11] F. Filippetti, M. Matrtelli, G. Francesschini, and C. Tassoni, "Development of expert system knowledge base to on-line diagnosis of rotor electrical faults of induction motors," in *Conf. Rec. 27th IEEE-IAS Annu. Meeting*, Oct. 1992, pp. 92–99.

[12] Z. Chaohai, M. Zongyuan, and Z. Qijie, "On-line incipient fault detection of induction motors using artificial neural networks," in *Proc. IEEE Int. Conf. Industrial Technology*, Dec. 1994, pp. 458–462.

[13] F. Filippetti, G. Francesschini, and C. Tassoni, "Neural networks aided on-line diagnostics of induction motor rotor faults," *IEEE Trans. Ind. Applicat.*, vol. 31, pp. 892–899, July/Aug. 1995.

[14] M.-y. Chow, R. N. Sharpe, and J. C. Hung, "On the application and design of artificial neural networks for motor fault detection," *IEEE Trans. Ind. Electron.*, vol. 40, pp. 181–197, Apr. 1993.

[15] P. V. Goode and M.-y. Chow, "Using a neural/fuzzy system to extract heuristic knowledge of incipient faults in induction motor," *IEEE Trans. Ind. Electron.*, vol. 42, pp. 131–146, Apr. 1995.

Xiang-Qun Liu received the B.S. degree from Beijing University of Aeronautics and Astronautics, Beijing, China.

From 1966 to 1974, she was an Engineer in the Beijing Electrical Motor Factory. Since 1974, she has been an Associate Professor in the Department of Automatic Control, Beijing University of Aeronautics and Astronautics. Her research interests include CAD of electrical motors, test and fault diagnosis of motors, and control of motor systems.

Hong-Yue Zhang (SM'91) received the B.S. degree from Beijing University of Aeronautics and Astronautics, Beijing, China.

From 1979 to 1981, he was a Visiting Scientist at Princeton University, Princeton, NJ, and at Houston University, Houston, TX. He has been a Visiting Professor at numerous universities worldwide. He is currently a Professor in the Department of Automatic Control, Beijing University of Aeronautics and Astronautics. His research interests include fault-tolerant control and navigation, fault detection and diagnosis, reliability of fault-tolerant systems, system identification and state estimation, and neural networks and their application. He has authored more than 100 papers and three books on his areas of research interest.

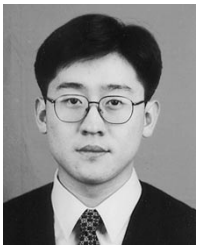

Jun Liu received the B.S. and M.S. degrees in electrical engineering from Beijing University of Aeronautics and Astronautics, Beijing, China, in 1995 and 1998, respectively.

He is currently with China Hewlett-Packard Company, Ltd., Beijing, China. His research interests include fault detection and diagnosis, and neural networks and their applications.

Jing Yang received the B.S. and M.S. degrees in electrical engineering in 1996 and 1998, respectively, from Beijing University of Aeronautics and Astronautics, Beijing, China, where she is currently working toward the Ph.D. degree in precision instrumentation and machinery.

Her research interests include fault detection and diagnosis, neural networks, and attitude determination with GPS and its applications.